Catalysis Today 156 (2010) 146–152

Contents lists available at ScienceDirect

Catalysis Today

journal homepage: www.elsevier.com/locate/cattod

Performances of tubular $La_{0.8}Sr_{0.2}Fe_{0.7}Ga_{0.3}O_{3-\delta}$ mixed conducting membrane reactor for under pressure methane conversion to syngas

Cédric Delbos*, Gilles Lebain, Nicolas Richet, Caroline Bertail

Air Liquide, Centre de Recherche Claude-Delorme, 1, Chemin de la Porte des Loges, 78354 Jouy-en-Josas Cedex, France

ARTICLE INFO

Article history:
Available online 12 June 2010

Keywords:
Methane
Syngas
MIEC (Mixed Ionic and Electronic Conductor)
Partial oxidation
Catalytic membrane reactor

ABSTRACT

The performances of the Mixed oxygen Ion and Electronic Conducting (MIEC) membrane reactor with surface catalyst was investigated for the methane conversion to synthesis gas, at operating conditions as close as possible to industrial requirements (pressurized syngas, high temperature, $CH_4 + H_2O$ mixture as feed). A dense self supported tubular membrane in one closed end geometry, made from the perovskite composition $La_{0.8}Sr_{0.2}Fe_{0.7}Ga_{0.3}O_{3-\delta}$ (LSFG), was elaborated by isostatic pressing and was coated with a $La_{0.8}Sr_{0.2}Fe_{0.7}Ni_{0.3}O_{3-\delta}$ (LSFN) porous catalyst.

Results show that LSFG membrane can be operated under pressure and pure methane as dry feed for more than 142 h without any fracture. Moreover, syngas production ($X(CH_4)$ and $S(CO)$) are greatly related to the reactor design and feed contact time. As a result, CH_4 conversion, CO selectivity, and oxygen permeation flux through the membrane can reach respectively 74%, 50% and 0.9 N m^3/m^2 h at 1173 K, with $CH_4 + H_2O$ mixture, S/C = 1 (Steam/Carbon ratio), P_{Feed} = 0.3 MPa and a feed contact time of 13 s.

Microstructure observations have shown Ni metallic exudation from LSFN surface catalyst and strontium rich continuous layer at catalyst/membrane interface under working conditions. However, these chemical/structural modifications did not seem to be detrimental to performances during short test duration (142 h).

1. Introduction

Numbers of companies are working on the production of syngas (H_2 and CO) using methane. Currently, steam methane reforming (SMR) is the most commonly used process for large-scale industrial synthesis gas production (syngas-mixture of hydrogen and carbon monoxide) [1]. The reactors are working in the temperature range 973–1223 K and under high pressure (2–4 MPa). Temperatures close to, or higher than 1073 K were nevertheless required to achieve a significant conversion to CO_x and H_2 (e.g., H_2 yields around 70%). However, a high consumption of energy is necessary due to the high endothermic nature of the reaction and the need to use excess steam to prevent from carbon formation.

An alternative process to produce hydrogen is the partial oxidation of methane (POM) using pure oxygen in the presence of a catalyst. This has greater selectivity and exothermicity [2]. Furthermore, the POM is kinetically faster than the steam reforming [3]. An associated route is the autothermal reforming (ATR), a self-sustaining process combining the POM and steam reforming. The main difficulty with the POM processes lies in consumption of large quantities of expensive pure oxygen, which is produced by the cryogenic separation of air and representing up to 40% of the total cost [4,5]. In fact, nitrogen cannot be tolerated in the reaction zone because it would convert to NO_x [3].

Ceramic membranes made from mixed oxygen-ionic and electronic conducting (MIEC) perovskite oxides can selectively separate oxygen from air at elevated temperature, typically higher than 973 K [6]. These membranes are promising for use as pure oxygen feedstock for POM process. Over the past several years, extensive efforts have been focused on using the MIEC membranes to improve the performance of methane conversion processes, i.e. combining air separation and high temperature catalytic partial oxidation (CPO) into a single step for syngas production (mixture of H_2 and CO) [6]. As a result, numerous membranes and catalysts formulations have been tested in tubular and planar shape reactor [6,7]. Very high methane conversion levels have been reported with CO selectivity close to 100% especially when using a Ni or Rh based catalyst [6,8–18]. However, few laboratories have tested MIEC membrane under pure methane [8–11] and long term operation (>500 h) [8,10,12–14,19], and very few publications deal with tests under pressure [15,20,21] (see Table 1 for an overview).

* Corresponding author at: Air Liquide-CRCD, 1, Chemin de la Porte des Loges, 78354 Jouy-en-Josas Cedex, France. Tel.: +33 01 39 07 62 94; fax: +33 01 39 07 62 93.
E-mail address: cedric.delbos@airliquide.com (C. Delbos).

0920-5861/$ – see front matter © 2010 Elsevier B.V. All rights reserved.
doi:10.1016/j.cattod.2010.04.047

Table 1
Overview of experimental studies reported in literature on MIEC membrane reactor operated under pure methane as feed gas, under long term operation and under pressure.

Membrane/catalyst/test duration	Shape	Feed/P_{syng}	T°	JO_2	X(CH4)	S(CO)	Ref.
$Ba_{0.5}Sr_{0.5}Co_{0.8}Fe_{0.2}O_{3-\delta}$	Crossing tube L = 30 cm, OD = 8 mm, WT = 1.5 mm.	100%CH_4 shell side	1148 K	4.8 Nm^3/m^2 h	94%	95%	[8]
LiLaNiO/γAl_2O_3 500 h		Atm. Pres.					
$La_{0.7}Sr_{0.3}Ga_{0.6}Fe_{0.4}O_{3-\delta}/La_{06}Sr_{0.4}CoO_{3-\delta}$ NiO	Disk	100%CH_4 Atm. Pres.	1123 K	11.2 Nm^3/m^2 h	88%	100%	[9]
$La_{0.6}Ca_{0.4}Fe_{0.75}Co_{0.25}O_{3-\delta}$	Crossing tube L = 2.5 cm, WT = 0.25 mm.	100%CH_4 + ~3%H_2O shell side	1173 K	1.4 Nm^3/m^2 h	99%	83%	[10]
HT xeramix POX catalyst 1400 h		Atm. Pres.					
$La_{0.5}Sr_{0.5}Ga_{0.2}Fe_{0.8}O_{3-\delta}$ (WT = 150 μm) onto porous αAl_2O_3 substrate	Crossing tube αAl_2O_3 tube L = 6.4 cm, OD = 20 mm, WT = 2.5 mm.	100%CH_4 shell side	1123 K	0.2 Nm^3/m^2 h	97%	100%	[11]
0.1 wt%Rh/Al_2O_3 packed bed		Atm. Pres.					
$Sm_{0.15}Ce_{0.85}O_{1.9}$–$Sm_{0.6}Sr_{0.4}Fe_{0.7}Al_{0.3}O_{3-\delta}$ (WT = 0.5 mm) + 50 wt% $Sm_{0.5}Sr_{0.5}CoO_3$–50 wt% $Sm_{0.\ 15}Ce_{0.85}O_{1.9}$ (WT = 20 μm (air side))	Disk	21%CH_4/He	1223 K	2.6 Nm^3/m^2 h	98%	98%	[12]
LiLaNiO/γAl_2O_3 Piled on disk surface 1100 h		Atm. Pres.					
$Ba_{0.5}Sr_{0.5}Co_{0.8}Fe_{0.2}O_{3-\delta}$ LiLaNiO/γAl_2O_3 500 h	Disk	50%CH_4/He Atm. Pres.	1173 K	6.9 Nm^3/m^2 h	98.5%	93%	[13]
$BaCo_{0.4}Co_{0.8}Fe_{0.4}Zr_{0.2}O_{3-\delta}$ Ni/La_2O_3-γAl_2O_3 >2000 h	Disk	50%CH_4/He Atm. Pres.	1123 K	3.2 Nm^3/m^2 h	96%	98%	[14]
$Ba_{0.5}Sr_{0.5}Co_{0.8}Fe_{0.2}O_{3-\delta}$ LiLaNiO/γAl_2O_3	Disk	25%CH_4/He 0.5 MPa on air side	1123 K	9.3 Nm^3/m^2 h	92%	90%	[15]
$La_{0.3}Sr_{1.7}Ga_{0.6}Fe_{1.4}O_{5.15}/La_{0.8}Sr_{0.2}CoO_3$ coating Ni/$La_{0.8}Sr_{0.2}MnO_3$ 1 year	Tube closed at one end	80%CH_4/He Atm. Pres.	1173 K		70%	99%	[19]
$LaSrFeCrO_x$/ Wrapped with foamed porous nickel	Tube closed at one end L = 12.8 cm, OD = 10.2 mm, WT = 1 mm.	10%H_2 + 10%CO + 40%CH_4 + 40%CO_2 + S/C ~ 1 shell side 1.38 MPa	1213 K	9.6 Nm^3/m^2 h	95%		[20]

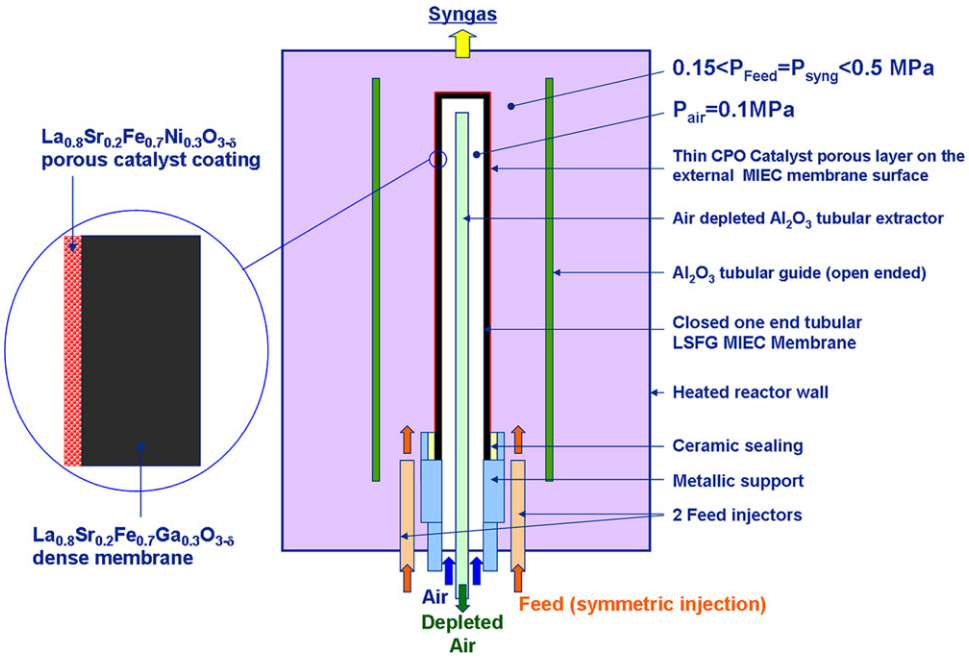

Fig. 1. Schematic diagram of the catalytic membrane reactor for methane conversion to syngas under pressure (0.15–0.5 MPa): air on core side and feed on shell side.

The goal of this work is to evaluate syngas production using $La_{0.8}Sr_{0.2}Fe_{0.7}Ga_{0.3}O_{3-\delta}$ membrane coated with $La_{0.8}Sr_{0.2}Fe_{0.7}Ni_{0.3}O_{3-\delta}$ porous catalyst. Operating conditions will be set as close as possible to industrial requirements (Dry Feed = 100%CH_4, 923–1173 K, $P_{Feed}(CH_4 + H_2O) = P_{Syngas} \sim 2$–4 MPa).

2. Experimental

Tubular membranes, closed at one end are manufactured by isostatic pressing. Dense, self supported membranes, of ~26 cm in length, and external diameter ~8.8 mm with a membrane thickness of ~0.7 mm are obtained after sintering at 1623 K during 2 h. The membrane formulation is the following: $La_{0.8}Sr_{0.2}Fe_{0.7}Ga_{0.3}O_{3-\delta}$ (LSFG).

A porous catalyst $La_{0.8}Sr_{0.2}Fe_{0.7}Ni_{0.3}O_{3-\delta}$ (LSFN) is deposited on the outside of the membrane (permeate side) by dip coating. Good adhesion and porous structure with a large exchange surface area is obtained after a short thermal treatment during 1 h at a temperature slightly below the sintering temperature.

Tubular membranes with outside catalyst layer were tested at 1173 K to produce syngas in the reactor described on Fig. 1. Air is used as the oxygen rich gas in the core side of the membrane and CH_4/Ar mixture as feed on the shell side. In order to prevent carbon formation in the reactor, steam is added to the feed mixture. A constant Steam/Carbon ratio (S/C) of 1 is maintained during the all test. Air side is maintained at atmospheric pressure (0.1 MPa) while the pressure on the feed side is set at 0.3 MPa. As shown on Fig. 1 the membrane is connected to the reactor using a high temperature ceramic sealing. This implies a very small temperature gradient along the membrane and maximizes the surface of active membrane. The maximum temperature gradient along the membrane is about 100 K (1173 ± 100 K over 26 cm). No leaks were detected during the all duration of the test and the carbon balance in the experiments performed was (100 ± 5%).

The inlet and outlet gas flow rates, the oxygen content in the depleted air and the dry syngas composition are monitored. The syngas product was analyzed every fifteen minutes by gas chromatography (Varian 3380). The oxygen content was on-line monitored with a Servomex oxygen analyzer Model 370A.

The performances of the catalytic membrane reactor are estimated using the following parameters: the oxygen permeation flux through the membrane (JO_2), the methane conversion ($X(CH_4)$), the carbon monoxide selectivity (S(CO)) and the hydrogen/carbon monoxide ratio (H_2:CO).

The methane conversion was calculated as:

$$X(CH_4) = \frac{QCH_4\text{feed} - QCH_4\text{syngas}}{QCH_4\text{feed}} \times 100\% \quad (1)$$

With Qi = flow rates of component *i* in Nm^3/h.

The selectivity of carbon monoxide formation was calculated as:

$$S(CO) = \frac{QCO\text{syngas}}{QCO\text{syngas} + QCO_2\text{syngas}} \times 100(\%) \quad (2)$$

The hydrogen carbon monoxide ratio was calculated as:

$$H_2 : CO = \frac{QH_2\text{syngas}}{QCO\text{syngass}}(\%) \quad (3)$$

The methane oxygen ratio was calculated as:

$$CH_4 : O_2 = \frac{QCH_4\text{feed}}{QO_2\text{membrane}}(\%) \quad (4)$$

With $QO_2\text{membrane} = QO_2\text{air} - QO_2\text{depleted air}$.

The oxygen permeation flux through the membrane was calculated as:

$$JO_2 = \frac{QO_2\text{membrane}}{\text{membane surface area}}(Nm^3/m^2\,h) \quad (5)$$

The feed contact time was calculated in real operating conditions ($T_{reactor}$, P_{feed}) as:

$$\text{Feed contact time} = \text{CtFeed} = \frac{Vol_{reactor}}{Q\text{feed}}(s) \quad (6)$$

With $Vol_{reactor}$ = enclosed volume between the alumina tubular guide and the membrane above the ceramic sealing.

The microstructure and EDS characterization of fresh and aged samples were achieved on FESEM Zeiss Ultra 55 associated with Bruker EDS microanalysis.

The calculation of the gaseous composition at thermodynamic equilibrium was done in Aspen-Hysys environment for fixed values

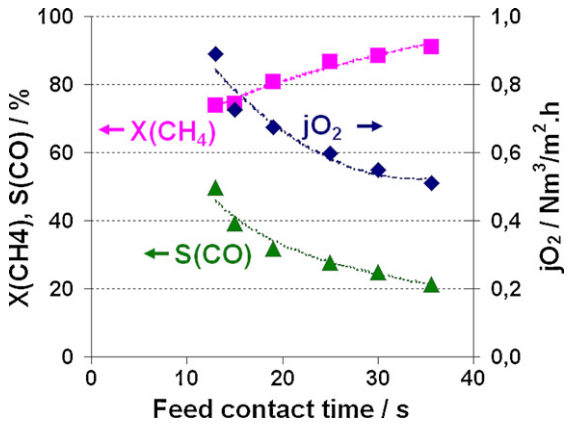

Fig. 2. Dependence of the methane conversion, carbon monoxide selectivity and oxygen permeation flux versus feed contact time under 100%CH_4 and S/C = 1 at 1173 K and P_{Feed} = 0.3 MPa.

of temperature and pressure and different mixture compositions. The components taken into account for the calculation are: methane, water, carbon monoxide, carbon dioxide, hydrogen and oxygen. The fluid package used to calculate the thermodynamic properties of the mixture is PRSV (Peng-Robinson equation of state modified by Stryjek and Vera [22]). A Gibbs free energy minimization method was used through a Gibbs reactor model [23]. With the free enthalpy procedure, individual equilibria are not considered as such. Rather, the products liable to be formed are noted, and the distribution of these species is established using a perfectly general mathematical technique to give a minimum Gibbs free enthalpy for the system at given conditions could then be achieved that would be known to satisfy all expected equilibria and be accurate within the limits of the thermodynamic data.

3. Results and discussion

Chemical reactions are governed by the thermodynamics of their reaction equilibrium. In a system where there is more than one reaction equilibrium there may be several routes to the desired products and by-products. The catalytic partial oxidation of methane constitutes such a system. Six major reactions are considered in this study, including the complete (7) or partial oxidation of methane (8), the steam (9) or dry methane reforming (10), the water gas shift (11) as well as carbon monoxide oxidation (12) reactions as follows:

$$CH_4 + 2O_2 \rightarrow CO_2 + 2H_2O, \quad \Delta H^0_{298\,K} = -802\,kJ/mol \tag{7}$$

$$CH_4 + \tfrac{1}{2}O_2 \rightarrow CO + 2H_2, \quad \Delta H^0_{298\,K} = -36\,kJ/mol \tag{8}$$

$$CH_4 + H_2O_2 \leftrightarrow CO_2 + H_2, \quad \Delta H^0_{298\,K} = +206\,kJ/mol \tag{9}$$

$$CH_4 + CO_2 \leftrightarrow 2CO + 2H_2, \quad \Delta H^0_{298\,K} = +247\,kJ/mol \tag{10}$$

$$CO + H_2O \leftrightarrow CO_2 + H_2, \quad \Delta H^0_{298\,K} = -41\,kJ/mol \tag{11}$$

$$CO + \tfrac{1}{2}O_2 \leftrightarrow CO_2, \quad \Delta H^0_{298\,K} = -257\,kJ/mol \tag{12}$$

Under pure methane, oxygen permeation flux through the membrane, CH_4 conversion and CO selectivity exhibit large variations versus feed contact time (feed flow rate) (Fig. 2).

As expected, the oxygen permeation flux through the membrane increases with shorter contact time (Fig. 2). In fact, JO_2 is linked to the oxidations reactions which maintain the oxygen partial pressure artificially low. Now the kinetics of methane oxidation reactions (10^{-2} to 10^{-4} s) [3] are not restrictive and therefore allow very fast contact time (<1 s). Consequently, from the oxygen partial pressure gradient point of view, the restrictive factor is the methane flow rate and then the feed contact time.

The selectivity to carbon monoxide formation increases with shorter contact time (Fig. 2). The CO selectivity ratio expresses the CO/CO_2 balance in the syngas. This gives an idea on the reactions occurring in the reactor: methane partial oxidation (8) and steam methane reforming (9) produces CO (↗S(CO)), dry reforming (10) consumes CO_2 and produces CO (↗↗S(CO), combustion (7) produces CO2 (↘S(CO) and Shift (11) as well as carbon monoxide oxidation consumes CO and produces CO_2 (↘↘S(CO). Combustion reaction is favored at low contact time while partial oxidation impact increases progressively with faster contact time.

In the case of methane conversion, it decreases with shorter contact time (Fig. 2) despite the experimental feed contact times range. This result could be explained by mass transfer restriction from gas to surface catalyst due to the laminar gas flow around the membrane, as well as the large gap (8.8 mm) between the Al_2O_3 guide and the perovskite membrane (Fig. 3). Shorter contact time lead to higher feed flow rate which increases the methane by-pass and therefore reduces the methane conversion.

As a result, CH_4 conversion, CO selectivity, and oxygen permeation flux through the membrane can reach respectively 74%, 50% and 0.9 N m^3/m^2 h at 1173 K, with $CH_4 + H_2O$ mixture, Steam (%mol)/Carbon (%mol) = 1, P_{Feed} = 0.3 MPa and a feed contact time of 13 s. Nevertheless, the experimental results are below the theoretical value calculated by Aspen-Hysys at thermodynamic equilibrium (Fig. 4). Such differences could be explained by mass transfer restriction and gas recirculation along the membrane due to the reactor design (Figs. 1 and 3), respectively in the case of the methane conversion and carbon monoxide selectivity.

Large contact time leads to very high H_2/CO ratio (Fig. 5). Pure partial oxidation would lead to H_2/CO ratio of 2 and pure steam reforming would lead to a value of 3. That means that other reactions take place in the reactor. CO oxidation and/or water gas shift

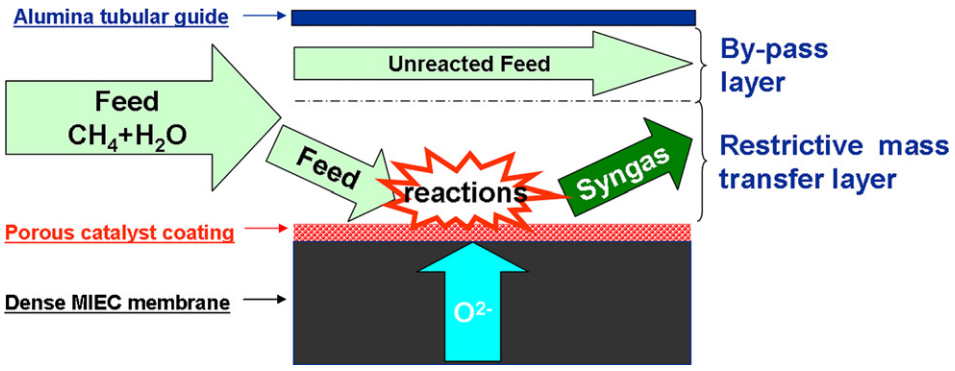

Fig. 3. Schematic diagram of the possible mass transfer restriction, from gas to surface catalyst, in the presented membrane reactor.

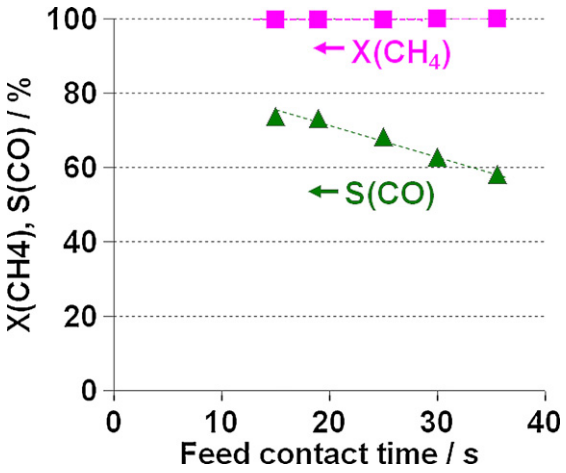

Fig. 4. Aspen-Hysys thermodynamic equilibrium simulation of the methane conversion and carbon monoxide selectivity versus feed contact time at 1173 K and P_{Feed} = 0.3 MPa, taking into account the measured feed and oxygen flows.

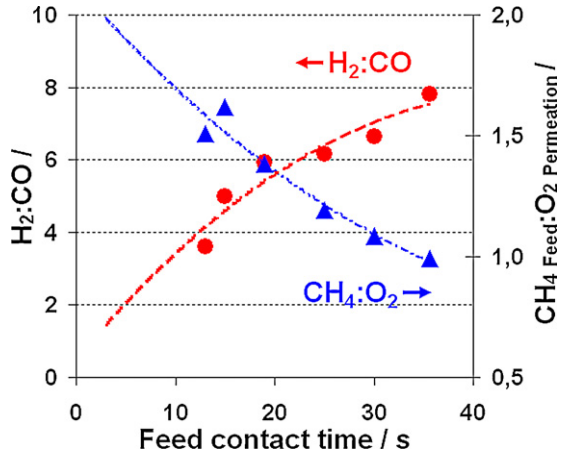

Fig. 5. Dependence of the H_2/CO and CH_4 feed/O_2 flow ratios versus feed contact time under 100%CH_4 and S/C = 1 at 1173 K and P_{Feed} = 0.3 MPa.

could explain such high H_2/CO ratio. Gas recirculation along the membrane, induced by the reactor design, could also explain such high value. An extrapolation for short contact time (<5 s) would lead to H_2/CO ratio close to 2 that is consistent with the results obtained by Bayraktar et al. [24] or Tong et al. [14]. It seems that a relation exists between H_2/CO ratio and CH_4 (feed)/O_2 (permeated). High CH_4/O_2 ratios are obtained at short contact time that is favorable for partial oxidation.

The reactor was operated for more than 142 h under pure methane, S/C = 1, 900 °C and P_{Feed} = 0.3 MPa.

The conversion of CH_4 to syngas using ceramic membrane is complicated to manage. Basically two reactions are in competition, combustion and reforming. From the experiments carried out in this work, it seems that the oxygen content in the mixture can indicate the major reaction. For rich O_2 mixture combustion is favored whereas reforming is favored for poor O_2 mixture. The difficulty is to control the oxygen amount in the reactor and especially on the surface of the membrane, where the reactions take place. Oxygen comes from the diffusion through the membrane that is controlled by the local oxygen partial pressure gradient, the surface exchange kinetics,. . . Those parameters are not directly under control during operation and can evolve during the test with the ageing of the membrane. The distribution of the reactants in the rector and the knowledge of membrane ageing are critical to keep the process under control. In our case, the dead volume around the membrane is very large. Assuming that most of the reactions take place at or near the surface of the membrane a large amount of methane does not react. The total conversion of methane is very low. That means that space between membranes should be reduced as much as possible to favor surface reactions and the oxygen flux through the membrane should be limited to maintain a CH_4/O_2 ratio favoring reforming reaction. Those results show that reactor design and membrane integration are key parameters to obtain good performance. Another solution could consist in filling the space between the alumina tubular guide and the porous catalyst coating with inert material or catalyst to generate some turbulence that would limit the by pass and promote more steam and dry reforming in the case volume catalyst.

Fig. 6 shows a surface observation and an EDS mapping of the membrane surface before test. The catalyst layer is porous with spherical agglomerates composed of submicron particles

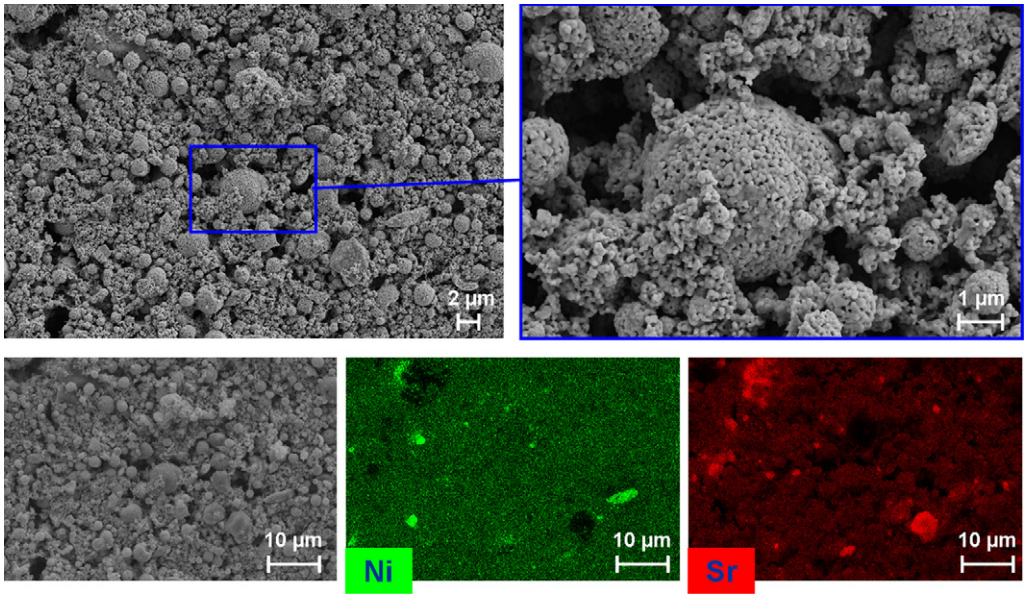

Fig. 6. FESEM observations and EDS mapping of fresh $La_{0.8}Sr_{0.2}Fe_{0.7}Ni_{0.3}O_{3-\delta}$ surface catalyst (after elaboration).

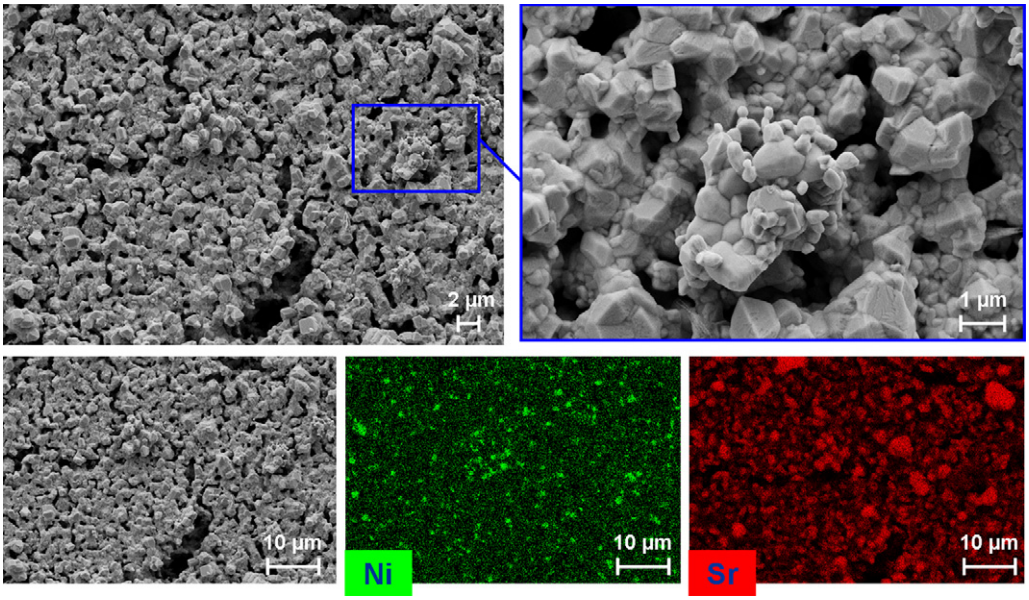

Fig. 7. FESEM observations and EDS mapping of aged $La_{0.8}Sr_{0.2}Fe_{0.7}Ni_{0.3}O_{3-\delta}$ surface catalyst (142 h 100%CH_4 dry feed – P_{Feed} = 0.3 MPa).

(~100 nm) coming from the manufacturing process. It is important to optimize coating adhesion but also to maintain a large porosity. EDS mapping indicate a pretty homogeneous distribution of Ni and Sr that is relevant with the initial perovskite formulation LSFN.

Fig. 7 shows the same membrane after tests. It is clear that the microstructure of the catalyst layer has been affected. The spherical agglomerates are not anymore visible and the coating seems denser. This densification induces cracks formation. However the catalyst layer is not fully dense and no modifications in term of oxygen flux, conversion or selectivity can be attributed to this evolution. EDS mapping indicates a segregation of Ni and Sr elements at the surface under reducing atmosphere. Nickel particles up to 1 μm are observed indicating that Ni was not fully stabilize by the perovskite structure under operating conditions.

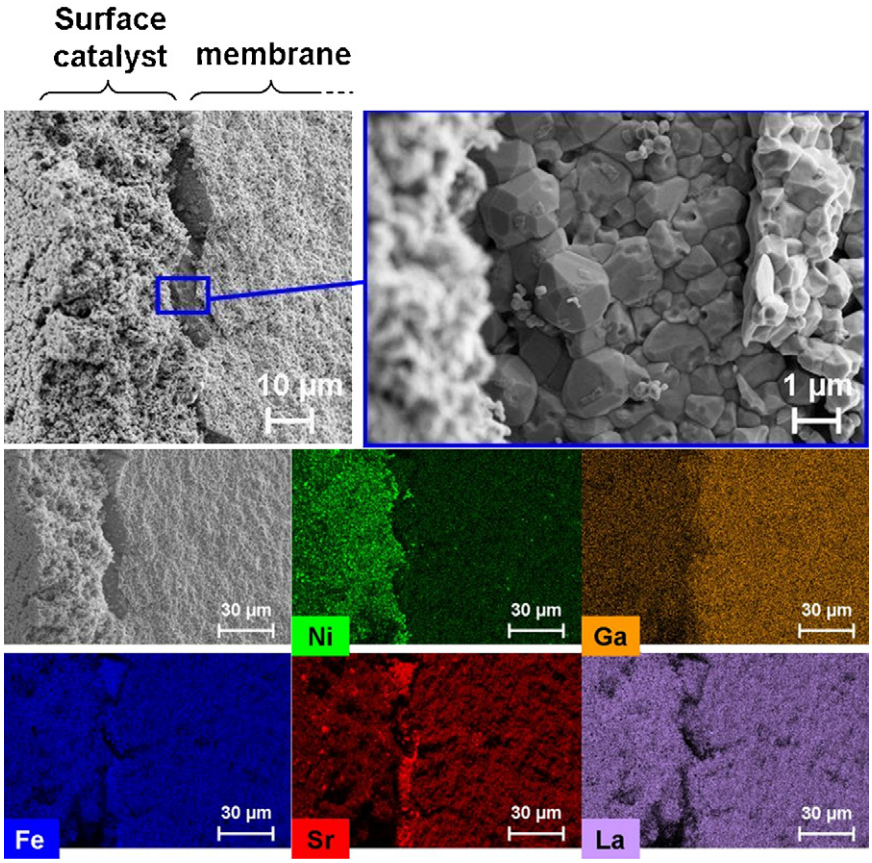

Fig. 8. FESEM observations and EDS mapping of a fracture cross section of LSFG/LSFN membrane after test (142 h 100%CH_4 dry feed – P_{Feed} = 0.3 MPa).

Fracture cross section observations (Fig. 8) put in evidence the formation of a 1–5 μm rich strontium intermediate layer between the MIEC membrane and the catalyst layer. Similar observations were done by Tong et al. [14] or Schwartz et al. [19] respectively on $BaCo_{0.4}Fe_{0.4}Zr_{0.2}O_{3-\delta}$ and on $La_{0.3}Sr_{1.7}Fe_{1.4}Ga_{0.6}O_{5.15}$. Those membranes exhibit metal oxides and carbonates (cobalt or strontium carbonate) formation on the permeate side. However, in both cases, the perovskite structure is still present over the all thickness of the membrane. The formation of the Sr rich dense layer does not affect the performances. Nowadays, it is not clear if this layer is made from Sr carbonates.

No carbon formation was detected in the reactor, probably due to steam injection and/or oxygen permeation through the membrane.

4. Conclusions

LSFG/LSFN membrane was operated successfully with a P_{Feed} of 0.3 MPa, pure methane dry feed, S/C ∼ 1 at 1173 K, for more than 142 h without any fracture. Methane conversion and CO selectivity are greatly related to the reactor design and feed contact time. Short contact time leads to better CO selectivity probably due to the excess of CH_4 compare to O_2. The ratio CH_4/O_2 seems to be the key parameter to control the reactions that take place in the reactor. As the performances of the membrane and the reactor design can have an impact on the evolution of the CH_4/O_2 ratio it is of great importance to understand the phenomenons involved and there evolution.

Important microstructural and chemical evolutions of both catalyst surface and membrane interface were observed. However, it seems that those evolutions have very limited impact on the performances of the catalytic membrane reactor during short duration test (142 h). Those evolutions must be evaluated over longer duration >1000 h to be representative of the industrial processes.

Acknowledgements

The authors would like to express their gratitude to the French environment and energy management agency (ADEME) for their financial support and the Center for Technology Transfers in Ceramics (CTTC France) for providing the ceramic membranes.

References

[1] J.G. Seo, M.H. Youn, K.M. Cho, S. Park, J.K. Song, J. Power Sources 173 (2007) 943.
[2] D.A Hickman, L.D. Schmidt, Science 259 (1993) 343.
[3] A. Kleinert, A. Feldhoff, T. Schiestel, J. Caro, Catal. Today 118 (2006) 44.
[4] K. Aasberg-Petersen, J.H. Bak Hansen, T.S. Christensen, I. Dybkjaer, P. Seier Christensen, C. Stub Nielsen, S.E.L. Winter Madsen, J.R. Rostrup-Nielsen, Appl. Catal. A: Gen. 221 (2001) 379.
[5] A.A. Yaremchenko, V.V. Kharton, A.A. Valente, F.M.M. Snijkers, J.F.C. Cooymans, J.J. Luyten, F.M.B. Marques, J. Membr. Sci. 319 (2008) 141.
[6] H.J.M. Bouwmeester, Catal. Today 82 (2003) 141.
[7] X. Dong, Z. Liu, W. Jin, N. Xu, J. Power Sources 185 (2008) 1340.
[8] H. Wang, Y. Cong, W. Yang, Catal. Today 82 (2003) 157.
[9] J.M. Kim, G.J. Hwang, S.H. Lee, C.S. Park, J.W. Kim, Y.H. Kim, J. Membr. Sci. 250 (2005) 11.
[10] S. Diethelm, J. Sfeir, F. Clemens, J.V. Herle, D. Favrat, J. Solid State Electrochem. 8 (2004) 611.
[11] J.T Ritchie, J.T. Richardson, D. Luss, AIChE J. 47 (2001) 2092.
[12] X. Zhu, Q. Li, Y. Cong, W. Yang, Catal. Commun. 10 (2008) 309.
[13] Z. Shao, H. Dong, G. Xiong, Y. Cong, W. Yang, J. Membr. Sci. 183 (2001) 181.
[14] J. Tong, W. Yang, R. Cai, B. Zhu, L. Lin, Catal. Lett. 78 (2002) 129.
[15] H. Lu, J. Tong, Y. Cong, W. Yang, Catal. Today 104 (2005) 154.
[16] U. Balachandran, J.T. Dusek, R.L. Mieville, R.B. Poeppel, M.S. Kleefisch, S. Pei, T.P. Kobylinski, C.A. Udovich, A.C. Bose, Appl. Catal. A/Gen. 133 (1995) 19.
[17] U. Balachandran, J.T. Dusek, P.S. Maiya, B. Ma, R.L. Mieville, M.S. Kleefisch, C.A. Udovich, Catal. Today 36 (1997) 265.
[18] M. Ikeguchi, T. Mimura, Y. Sekine, E. Kikuchi, M. Matsukata, Appl. Catal. A: Gen. 290 (2005) 212.
[19] M. Schwartz, J.H. White, A.F. Sammells, WO21649 (1999).
[20] C.J. Besecker, T.J. Mazanec, S.J. Xu, E. Rytter, US 7125528 (2006).
[21] M.F. Carolan, US 7468092 (2008).
[22] R. Stryjek, J.H. Vera, Can. J. Chem. Eng. 64 (1986) 820.
[23] W.B. White, S.M. Johnson, G.B. Dantzig, J. Chem. Phys. 28 (1958) 751.
[24] D. Bayraktar, F. Clemens, S. Diethelm, T. Graule, J.V. Herle, P. Hotappels, J. Eur. Ceram. Soc. 27 (2007) 2455.